

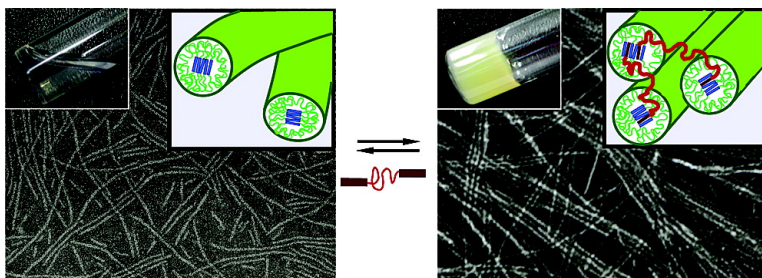
Communication

## Transformation of Isotropic Fluid to Nematic Gel Triggered by Dynamic Bridging of Supramolecular Nanocylinders

Ja-Hyoung Ryu, and Myongsoo Lee

*J. Am. Chem. Soc.*, **2005**, 127 (41), 14170-14171 • DOI: 10.1021/ja055583x • Publication Date (Web): 27 September 2005

Downloaded from <http://pubs.acs.org> on March 25, 2009



### More About This Article

Additional resources and features associated with this article are available within the HTML version:

- Supporting Information
- Links to the 6 articles that cite this article, as of the time of this article download
- Access to high resolution figures
- Links to articles and content related to this article
- Copyright permission to reproduce figures and/or text from this article

[View the Full Text HTML](#)

## Transformation of Isotropic Fluid to Nematic Gel Triggered by Dynamic Bridging of Supramolecular Nanocylinders

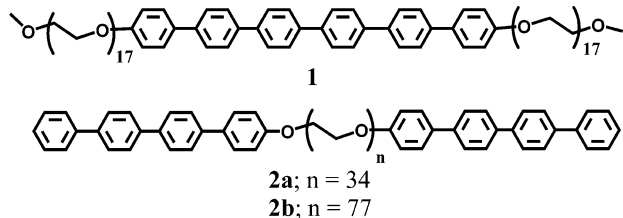
Ja-Hyoung Ryu and Myongsoo Lee\*

Center for Supramolecular Nano-Assembly and Department of Chemistry, Yonsei University, Seoul 120-749, Korea

Received August 16, 2005; E-mail: mslee@yonsei.ac.kr

Spontaneous formation of supramolecular architectures by self-assembly of amphiphilic molecules is of great interest in areas ranging from chemistry, biology, to materials science, driven by a wide variety of potential applications.<sup>1</sup> Extensive efforts thus have been directed toward functional supramolecular systems for exploration of novel properties and functions that are difficult without specific assembly of molecular components.<sup>2</sup> Self-assembling molecules based on *p*-conjugated rods are receiving increased attention as building blocks for electrooptically active supramolecular structures, such as discrete bundles, cylinders, and vesicles.<sup>3</sup> Recently, we have shown that incorporation of a conjugated rod into an amphiphilic dumbbell-shaped molecular architecture gives rise to the formation of a helical nanostructure, consisting of hydrophobic aromatic cores surrounded by hydrophilic flexible segments that are exposed to the aqueous environment.<sup>4</sup>

We present here the formation of discrete nanocylinders from the self-assembly of a coil-rod-coil molecule (**1**) based on a conjugated rod segment in aqueous solution and reversible bridging between nematic gel and isotropic fluid triggered by addition of a rod-coil-rod molecule (**2b**) in hierarchical self-assembly of supramolecular nanocylinders (Figure 1). The coil-rod-coil molecule (**1**) that forms the cylindrical aggregates consists of a hexa-*p*-phenylene rod and poly(ethylene oxide) chains (DP = 17) that are covalently linked at both ends of the rod segment. The synthesis of the coil-rod-coil molecule started with a stepwise fashion according to the procedure described previously.<sup>5</sup> The rod-coil-rod molecules were synthesized by etherification of a ditosylated poly(ethylene oxide) with 4-hydroxy-4'-bromo-biphenyl and aromatic coupling with aryl boronic acid. The resulting molecules were characterized by <sup>1</sup>H and <sup>13</sup>C NMR spectroscopy, elemental analysis, and MALDI-TOF mass spectroscopy and are shown to be in full agreement with the structures presented.



The coil-rod-coil molecule (**1**), when dissolved in a selective solvent for one of the blocks, can self-assemble into an aggregate structure because of its amphiphilic characteristics. **1** was observed to self-assemble into discrete spherical micelles at the initial stage. However, these micelles were shown to slowly change into cylindrical objects on time scale of a week, indicating that cylindrical aggregates are thermodynamically stable objects in this system.<sup>6</sup> Dynamic light scattering (DLS) experiments were performed with **1** in aqueous solution (0.1 wt %) in order to investigate the aggregation behavior.<sup>7</sup> The CONTIN analysis of the autocor-

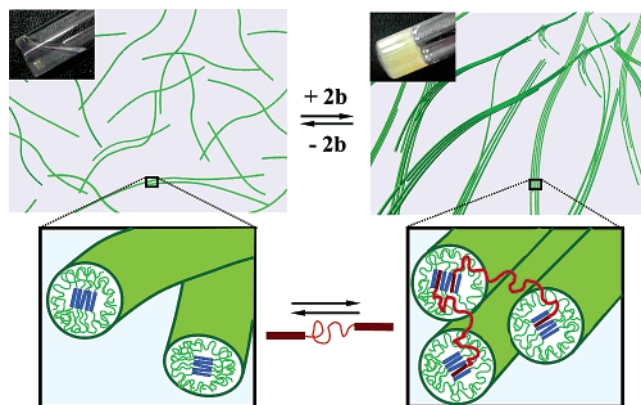


**Figure 1.** Schematic representation of reversible bridging between isotropic fluid and nematic gel of supramolecular nanocylinders.

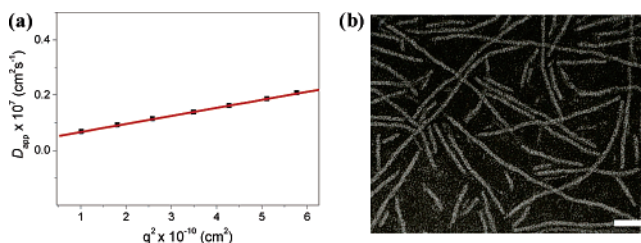


**Figure 2.** (a) Angular dependence of the apparent diffusion coefficient for **1** aqueous solution (0.1 wt %) and (b) TEM image of **1** with negative staining (0.01 wt %, scale bar = 50 nm).

relation function shows a broad peak corresponding to an average hydrodynamic radius of approximately 158 nm. The angular dependence of the apparent diffusion coefficient ( $D_{app}$ ) was measured because the slope is related to the shape of the diffusing species (Figure 2a). The slope was observed to be 0.03, consistent with the value predicted for cylindrical micelles.<sup>8</sup> The formation of cylindrical micelles was further confirmed by the Kratky plot that shows a linear angular dependence over the scattering light intensity of the aggregates.<sup>9</sup>

The evidence for the formation of the cylindrical aggregates was also provided by transmission electron microscopy (TEM) experiments. The micrographs with negative stained samples show cylindrical aggregates with a uniform diameter of about 10 nm and lengths up to several hundreds of nanometers (Figure 2b). Considering the extended molecular length (13 nm by CPK), the image indicates that the diameter of the elementary cylindrical objects corresponds to one molecular length.

Remarkably, addition of **2b** at the concentrations from 2 to 30 wt % relative to **1** induces anisotropic gelation in the isotropic fluid phase of **1** (Figure 3a).<sup>10</sup> In the case of addition of 10 wt % of **2b** relative to **1**, for example, the isotropic solution undergoes spontaneous anisotropic gelation even at a total concentration as low as 2.5 wt %. More importantly, the resulting gel was shown to

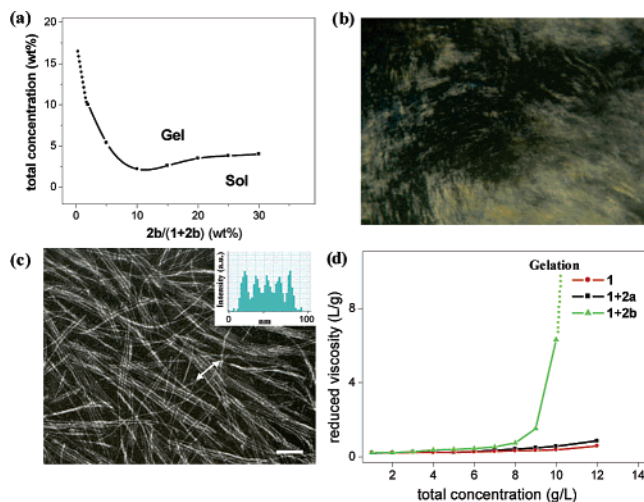


**Figure 3.** (a) Phase diagram plotted in terms of the total concentration versus the concentration of **2b** in the total amphiphilic molecules (**1** + **2b**), (b) a representative optical polarized micrograph of nematic gel phase, and (c) TEM image of nematic gel with 10 wt % **2b** relative to **1**, with density profile inset (scale bar = 100 nm). (d) Reduced viscosities of solution of **1** and 10 wt % **2a** and **2b** relative to **1** versus concentration in water at 25 °C.

reversibly transform into a transparent fluid solution, upon slight reduction in the amount of **2b** from the gel. The polarized optical micrograph (POM) of this reversible gel shows a threadlike texture, characteristic of a nematic structure (Figure 3b).<sup>2b</sup> In the gel state, the SAXS patterns showed a single broad peak centered at  $d$ -spacing of 14 nm, corresponding to the distance between the cylinders in the nematic structure, and the wide-angle X-ray scattering patterns showed the peak at  $q = 14 \text{ nm}^{-1}$  associated with inter-rod distance within the cylindrical micelles together with the two water peaks at 20 and  $27 \text{ nm}^{-1}$ .

As shown Figure 3c, TEM performed with the solution of 10 wt % **2b** relative to **1** shows bundles of the cylindrical micelles aligned in a parallel fashion, in contrast to the solution of **1**. The density profiles taken perpendicular to the long axis of the bundle show inter-cylinders distance to be about 14 nm (Figure 3c, inset); that is consistent with the SAXS result. These results demonstrate that addition of **2b** into the solution of **1** drives the isotropic solution of the cylindrical micelles to the nematic gel state in which the cylindrical micelles are aligned parallel to each other to form rigid bundles. These bundles are likely to be responsible for the formation of the anisotropic gel.

This result can be rationalized by considering the bridging of the individual cylindrical micelles into bundles through coassembly with **2b**. The aromatic moieties of rod-coil-rod molecule **2b** will coassemble into the aromatic cores of the cylindrical micelles through hydrophobic and  $\pi$ - $\pi$  interactions.<sup>11</sup> As a result, the cylindrical micelles might be interconnected in enforced proximity to each other to form anisotropic gels (Figure 1). The coassembling behavior of **1** and **2b** was confirmed by using fluorescence spectroscopy. When the mixture solution of **1** and **2b** was excited at 290 nm, where most of the radiation is absorbed by **2b**, the emission spectrum exhibits only a strong maximum at 431 nm corresponding to **1** with a complete lack of the emission at 398 nm associated with the aromatic unit of **2b**.<sup>12</sup> This result indicates that energy transfer takes place between the aromatic units of **2b** and those of **1** within the supramolecular cylinders, demonstrating that the cylindrical micelles of **1** are effectively bound by **2b**.

To further investigate bridging of the cylinders, the viscosities of 1–15 g/L aqueous solutions of **1**, **1·2a**, and **1·2b**, respectively, were measured at 25 °C by means of a capillary viscosimeter (Figure 3d). By increasing the concentration, essentially no change in the viscosity was observed in the case of **1** and **1·2a** solutions. In great contrast, the viscosity of **1·2b** abruptly increases above a concentration of 8 g/L, indicative of the onset of effective bridging between adjacent cylindrical micelles. These results imply that the chain length of **2a** is too short to interconnect the supramolecular cylinders, while that of **2b** is sufficiently long to interconnect adjacent cylindrical micelles.<sup>13</sup> This strongly supports that, as expected, bridging the adjacent cylindrical micelles requires rod-coil-rod molecules above a certain coil length.

In summary, we have demonstrated that the cylindrical micelles self-assembled from coil-rod-coil molecules can be interconnected by addition of a small amount of rod-coil-rod molecule as a bridging agent. Subsequently, these dynamic interconnections lead to stiff bundles composed of cylindrical micelles that are responsible for the formation of a reversible nematic gel. The results described here represent a significant example that dynamic bridging of supramolecular cylinders in aqueous solution can provide a useful strategy to construct one-dimensional nematic structure with three-dimensional elastic properties.

**Acknowledgment.** This work was supported by the National Creative Research Initiative Program of the Korean Ministry of Science and Technology.

**Supporting Information Available:** Synthetic procedures, characterization, DLS and SLS, TEM, X-ray, POM data, and emission spectra. This material is available free of charge via the Internet at <http://pubs.acs.org>.

## References

- (1) (a) Lee, M.; Cho, B.-K.; Zin, W.-C. *Chem. Rev.* **2001**, *101*, 3869–3892. (b) Antonietti, M.; Förster, S. *Adv. Mater.* **2003**, *15*, 1323–1333. (c) Sarikaya, M.; Tamerler, C.; Jen, A. K. Y.; Schulten, K.; Baneyx, F. *Nat. Mater.* **2003**, *2*, 577–585.
- (2) (a) Ky Hirschberg, J. H. K.; Brunsveld, L.; Ramzi, A.; Vekemans, J. A. J. M.; Sijbesma, R. P.; Meijer, E. W. *Nature* **2000**, *407*, 167–170. (b) Kawano, S.-i; Fujita, N.; Shinkai, S. *J. Am. Chem. Soc.* **2004**, *126*, 8592–8593. (c) Kuroiwa, K.; Shibata, T.; Takada, A.; Nemoto, N.; Kimizuka, N. *J. Am. Chem. Soc.* **2004**, *126*, 2016–2021. (d) Enomoto, M.; Kishimura, A.; Aida, T. *J. Am. Chem. Soc.* **2001**, *123*, 5608–5609.
- (3) (a) Hoeben, F. J. M.; Jonkhijm, P.; Meijer, E. W.; Schenning, A. P. H. *J. Chem. Rev.* **2005**, *105*, 1491–1546. (b) Messmore, B. W.; Hulvat, J. F.; Sone, E. D.; Stupp, S. I. *J. Am. Chem. Soc.* **2004**, *126*, 14452–14458. (c) Varghese, R.; George, S. J.; Ajayaghosh, A. *Chem. Commun.* **2005**, 593–595. (d) Wang, H.; You, W.; Jiang, P.; Yu, L.; Wang, H. H. *Chem.-Eur. J.* **2004**, *10*, 986–993. (e) Lee, M.; Kim, J.-W.; Hwang, I.-W.; Kim, Y.-R.; Oh, N.-K.; Zin, W.-C. *Adv. Mater.* **2001**, *13*, 1363–1368. (f) Lee, M.; Jeong, Y.-S.; Cho, B.-K.; Oh, N.-K.; Zin, W.-C. *Chem.-Eur. J.* **2002**, *8*, 876–883.
- (4) Bae, J.; Choi, J.-H.; Yoo, Y.-S.; Oh, N.-K.; Kim, B.-S.; Lee, M. *J. Am. Chem. Soc.* **2005**, *127*, 9668–9669.
- (5) Lee, M.; Jang, C.-J.; Ryu, J.-H. *J. Am. Chem. Soc.* **2004**, *126*, 8082–8083.
- (6) Svenson, S.; Messersmith, P. B. *Langmuir* **1999**, *15*, 4464–4471.
- (7) See Supporting Information.
- (8) Massey, J.; Power, N.; Manners, I.; Winnik, M. A. *J. Am. Chem. Soc.* **1998**, *120*, 9533–9540.
- (9) (a) Boersma, S. *J. Chem. Phys.* **1981**, *74*, 16989. (b) Bockstaller, M.; Köhler, W.; Wegner, G.; Vlassopoulos, D.; Fytas, G. *Macromolecules* **2000**, *33*, 3951–3953.
- (10) It should be noted that pure **2b** self-assembles into stable spherical micelles with a diameter of 14 nm, irrespective of the solution concentrations.
- (11) (a) Tanaka, F. *Macromolecules* **1998**, *31*, 384–393. (b) Zhang, K.; Xu, B.; Winnik, M. A.; Macdonald, P. M. *J. Phys. Chem.* **1996**, *100*, 9834–9841.
- (12) Excitation of pure **2b** in aqueous solution (1 wt %) at 290 nm revealed the strong emission with a maximum at 398 nm.
- (13) (a) The extended molecular lengths of **2a** and **2b** are estimated to be about 14 and 25 nm by CPK, respectively. However, the end-to-end distances of the chains in aqueous solutions are believed to be much shorter due to random coil conformations. (b) Kim, M.; Choi, Y.-W.; Sim, J.-H.; Choo, J.; Sohn, D. *J. Phys. Chem. B* **2004**, *108*, 8269–8277.

JA055583X